Analytical and Bioanalytical Chemistry (2019) 411:6427–6434
https://doi.org/10.1007/s00216-019-02023-6

RESEARCH PAPER

Site-specific peak intensity ratio (SPIR) from 1D $^{2}H/^{1}H$ NMR spectra for rapid distinction between natural and synthetic nicotine and detection of possible adulteration

Bin Liu[1,2,3] · Yanli Chen[1,2] · Xiaofang Ma[1,2,3] · Kaifeng Hu[1,2]

Received: 26 April 2019 / Revised: 4 June 2019 / Accepted: 5 July 2019 / Published online: 19 July 2019

Abstract

^{1}H and ^{2}H NMR spectra of 4 natural and synthetic nicotine samples were collected in a non-quantitative way and *s*ite-specific $^{2}H/^{1}H$ *p*eak *i*ntensity *r*atio (SPIR) was calculated for 12 distinct sites of nicotine. Experimental results illustrated that the SPIRs at sites of 6, 2′, and 5′β of natural nicotine were significantly different from those of the synthetic nicotine, and could be used for nicotine authentication as the measured SPIRs were indicative of the site-specific natural isotope fractionation. We demonstrated that this method could be applied to detect adulteration of natural nicotine with as low as 20% synthetic nicotine, without the need to measure the site-specific δD values, which usually required time-consuming quantitative ^{2}H NMR and additional IRMS for the overall $^{2}H/^{1}H$ isotopic ratio determination. The distinguishable $^{2}H/^{1}H$ SPIRs of nicotine, which can be quickly measured by NMR in non-quantitative way, can serve as an attractive alternative tool for tobacco authentication.

Keywords ^{1}H and ^{2}H NMR spectra · Site-specific peak intensity ratio (SPIR) · Non-quantitative · Nicotine

Introduction

Isotope ratio mass spectrometry (IRMS) is widely used for isotope ratio analysis at natural abundance which provides isotope contents of elements such as $^{2}H/^{1}H$, $^{13}C/^{12}C$, $^{15}N/^{14}N$, $^{18}O/^{16}O$, and $^{34}S/^{32}S$ [1–5]. However, a major drawback of IRMS is that the compound must be first converted into a simple gas, such as H_2, CO_2, N_2, CO, and SO_2 [1, 4, 5], and only the overall isotope ratio among all sites of the molecule can be obtained. In the 1980s, the introduction of SNIF-NMR (site-specific natural isotope fractionation by nuclear magnetic resonance) technique [6], which can provide the direct access to site-specific isotope ratios of $^{2}H/^{1}H$ at natural abundance, was immediately recognized as a powerful technique to authenticate the origin of natural or synthetic products, such as vanillin [7, 8], linalool [9], and benzaldehyde [10], as well as to detect the addition of sugar to fruit juices and wines [11, 12]. In the applications above, the $^{2}H/^{1}H$ isotopic ratios were measured by the high-field quantitative ^{2}H NMR method, which is usually time-consuming. For example, on an 11.75-T spectrometer, it takes about 2 h to collect a quantitative ^{2}H NMR spectrum for analysis of a sample containing 500 mg vanillin [13], which is costly and an extremely high concentration in general. In other words, it will require about 200 h to collect such a quantitative ^{2}H NMR spectrum with comparable signal-to-noise ratio with the (S)-Nicotine (3-[(2S)-1-methylpyrrolidin-2-yl]pyridine) sample at much lower concentration in our study, which is obviously unpractical. In addition, an IRMS spectrometer is often required to determine the overall $^{2}H/^{1}H$ isotopic ratio. Here, we propose a novel and rapid non-quantitative NMR method to differentiate natural and synthetic nicotine by comparison of site-specific $^{2}H/^{1}H$ peak intensity ratios (SPIR) derived from ^{1}H and ^{2}H NMR spectra, without the need of measurement of the site-specific δD values.

Bin Liu and Yanli Chen contributed equally to this work.

Electronic supplementary material The online version of this article (https://doi.org/10.1007/s00216-019-02023-6) contains supplementary material, which is available to authorized users.

✉ Kaifeng Hu
kaifenghu@cdutcm.edu.cn

[1] Innovative Institute of Chinese Medicine and Pharmacy, Chengdu University of Traditional Chinese Medicine, No. 1166 Liutai Avenue, Wenjiang District, Chengdu 611137, Sichuan, China

[2] State Key Laboratory of Phytochemistry and Plant Resources in West China, Kunming Institute of Botany, Kunming 650201, Yunnan, China

[3] University of Chinese Academy of Sciences, Beijing 100049, China

Natural nicotine is the most abundant alkaloid isolated from the tobacco plant [14], which grows between 60° north and 40° south [15]. In recent research, nicotine and several of its analogues have shown therapeutic benefits for a number of diseases caused by nervous system disorders, including Parkinson's disease [16, 17] and Tourette's syndrome [18]. It has been reported that the natural (S) (−) nicotine is more potent than the synthetic (R) (+) counterpart [19]; thus, using the natural nicotine for treatment in general can be regarded as a strong advantage. But natural nicotine, being limited by geographical distribution, complex extraction process, and low yield [15], is prone to adulteration.

Previous studies reported that the pyridine ring of nicotine was biosynthesized from aspartic acid and glyceraldehyde-3-phosphate, while the precursors of the pyrrolidine ring were the amino acids of ornithine or arginine, and the N-methyl moiety was derived from S-adenosyl methionine [14, 20]. However, for synthetic nicotine, using different starting reactants, such as 3-pyridinecarboxaldehyde [21], 3-(3-pyridyl)allyl carbonates [22] for pyridine ring, and B-allyldiisopropylaminoboran and azide anion [21] for pyrrolidine ring, will result in different $^{2}H/^{1}H$ isotopic ratios, which can be characteristic used for identification of compounds derived from different origins or with different history of synthetic pathway. So, from the point of view of stable isotopic composition, nicotine can be considered as a model molecule for tobacco authentication.

Nicotine extracted from natural tobacco exhibits deuterium content at pyridine and pyrrolidine ring that is significantly different from that of synthetic nicotine since enzymatic and/or chemical processes are likely to induce different isotopic fractionation. Deuterium content has been illustrated to be the most discriminating parameter for identification of tobacco from different geographical origins [15]. The proposed NMR method discriminates natural from synthetic nicotine through direct comparison of $^{2}H/^{1}H$ SPIR values derived from ^{1}H and ^{2}H NMR spectra. $^{2}H/^{1}H$ peak intensity ratios at several characteristic sites in nicotine, at which natural nicotine has dramatically different isotopic composition from synthetic sample, can be used to unambiguously detect adulteration of natural nicotine with as low as 20% synthetic nicotine.

Materials and methods

Sample preparation

Two natural nicotine samples, *p*-Nicotine (*p*urified natural product, provided by Dr. Yaning Fu) and (S)-Nicotine (TRC, catalog number KIT0555) and 2 synthetic nicotine samples, (R)-Nicotine and *rac*-Nicotine (TRC, catalog numbers N412430 and N412420, respectively) were used in this study. *p*-, (S)-, (R)-, and *rac*-Nicotine samples were prepared by dissolving 50, 50, 29, and 35 mg of each sample, respectively, in nitromethane (CH_3NO2); A 2× *p*-Nicotine sample was prepared by dissolving 100 mg *p*-Nicotine in nitromethane, which was used to illustrate the measured $^{2}H/^{1}H$ NMR SPIR values of nicotine are independent of the nicotine concentration. Finally, an adulterated nicotine sample was prepared by dissolving 60 mg natural *p*-Nicotine and 14 mg synthetic *rac*-Nicotine in CH_3NO2, which was used to demonstrate the application of the proposed method to detect adulteration of natural nicotine with as low as 20% synthetic nicotine. The high concentrations of pure compounds used correspond to the typical conditions for isotope analysis. All solutions were made up to 500 μl and then transferred to 5-mm NMR tubes for NMR experiments.

NMR experiments and data processing

All NMR experiments were performed at 298 K on a Bruker Avance III 800 MHz spectrometer equipped with a QCI cryoprobe and Z-gradients. 1D ^{1}H spectrum was recorded with a sweep width of 8012 Hz, TD of 32 K, and a short non-quantitative interscan delay of 1 s. It is noteworthy that a small-angle excitation pulse was intentionally used with p1 of 0.33 μs to hold down the solvent peak, which can suppress the effect of radiation damping and alleviate the baseline distortion caused by solvent peak. It can thus significantly improve the accuracy of the integration of each individual peak. A total of 120 (NS) scans were accumulated in the fid data to increase signal-to-noise ratio, resulting in an experimental time of 7 min. 1D ^{2}H spectrum was recorded with GARP for ^{1}H decoupling, a sweep width of 1228 Hz, TD of 8 K, p1 of 150 μs for 90° excitation, and a short non-quantitative interscan delay of 0.8 s. A total of 7680 (NS) scans were accumulated in the fid data, resulting in an experimental time of 317 min. In contrast to the conventional 1D quantitative ^{2}H NMR for the measurement of the site-specific δD values for isotope analysis, much shorter experimental time is crucial to obtain a high precision, as fast experiments are less affected by hardware instabilities over time.

Data processing, including Fourier transformation and phase and baseline correction, was performed using MestRe Nova [23]. Solvent peak was used as chemical shift reference and adjusted to 4.33 ppm. Global spectral deconvolution (GSD) was used for peak fitting to obtain the peak intensities. Considering the bias or systematic error in the data processing step, NMR data for each sample were independently processed by different authors and used for subsequent multivariate data analysis.

Theoretical description

Although the measured NMR peak intensity ratios are not equal to the site-specific natural isotope fractionation (SNIF), they are indicative of different SNIF. For a given molecular site (i), the SPIR value, $(^{2}H/^{1}H)_i$ was calculated as,

$$\left(\frac{^{2}H}{^{1}H}\right)_i = \frac{^{2}H_i}{^{1}H_i} = {}^{2}H_{0,i} \times \left[f_{re,^{2}H_i} \times f_{e,^{2}H_i} \times f_{a,^{2}H_i} \times f_{r,^{2}H}\right] \Big/ {}^{1}H_{0,i} \times \left[f_{re,^{1}H_i} \times f_{e,^{1}H_i} \times f_{a,^{1}H_i} \times f_{r,^{1}H}\right] = C_i \times \frac{^{2}H_{0,i}}{^{1}H_{0,i}} \quad (i = 1\text{–}12) \tag{1}$$

where i represents 12 distinct sites of nicotine (Fig. 1), $^{2}H_i$ is the measured peak intensity of the signal of site i in ^{2}H spectrum, and $^{1}H_i$ is the corresponding peak intensity of site i in ^{1}H spectrum of the same sample. $^{2}H_{0,i}$ and $^{1}H_{0,i}$ denote site-specific natural isotope fractionation of ^{2}H and ^{1}H at site i, respectively. The detected site-specific peak intensities $^{2}H_i$ and $^{1}H_i$ (that is, the detected current intensities in the probe coil or FIDs) are proportional to the isotope fractionation $^{2}H_{0,i}$ and $^{1}H_{0,i}$, respectively, but affected by multiple factors, including the recovery extent to the equilibrium (f_{re}), the exciting efficiency factor (f_e), the NMR signal attenuation factor (f_a) [24], and the receiving efficiency factor (f_r) [25]. Factors f_{re}, which depend on the interscan delay and the T_1 relaxation properties of nuclei ^{2}H or ^{1}H at specific site of nicotine, are site-specific constants when ^{2}H or ^{1}H experimental parameters are same among all samples. Factors f_e depend on the excitation pulse length and off-resonance effect of specific nuclei ^{2}H or ^{1}H. For example, f_e can be approximated to be 1 for 90° excitation or a much smaller but constant value for excitation with a very short p1 of 0.33 μs when the off-resonance effect is negligible as in the case of 1D ^{2}H and ^{1}H experiments. Signal attenuation factors f_a depend on the T_2 relaxation properties of specific nuclei at site i ($R_{2,i}$) and the duration of the pulse sequence (T), which can be generalized as.

$$f_{a,^{2}H_i}/{}^{1}H_i = e^{-\sum R_{2,i} \times T} \tag{2}$$

For direct 1D ^{2}H and ^{1}H experiments, FIDs are recorded immediately after the excitation pulse, f_a can be approximated to be 1 because the duration of the pulse sequence T is close 0. Factors f_r, which are dominantly affected by the solution permittivity (such as, the salt concentration), can be assumed to be nucleus-specific constants for ^{2}H and ^{1}H if solution conditions are maintained consistent among all samples.

Overall, all these factors for ^{2}H and ^{1}H spectra can be consolidated as a generalized site-specific constant C_i, which accounts for the proportionality of the measured SPIR values with regard to the authentic SNIF values. For samples with consistent solution conditions, constant C_i is site-specific but invariant among all samples when 1D ^{1}H and ^{2}H spectra were recorded with the same pulse sequences and identical parameters. Therefore, the measured SPIR values are directly indicative of the authentic SNIF values of each sample.

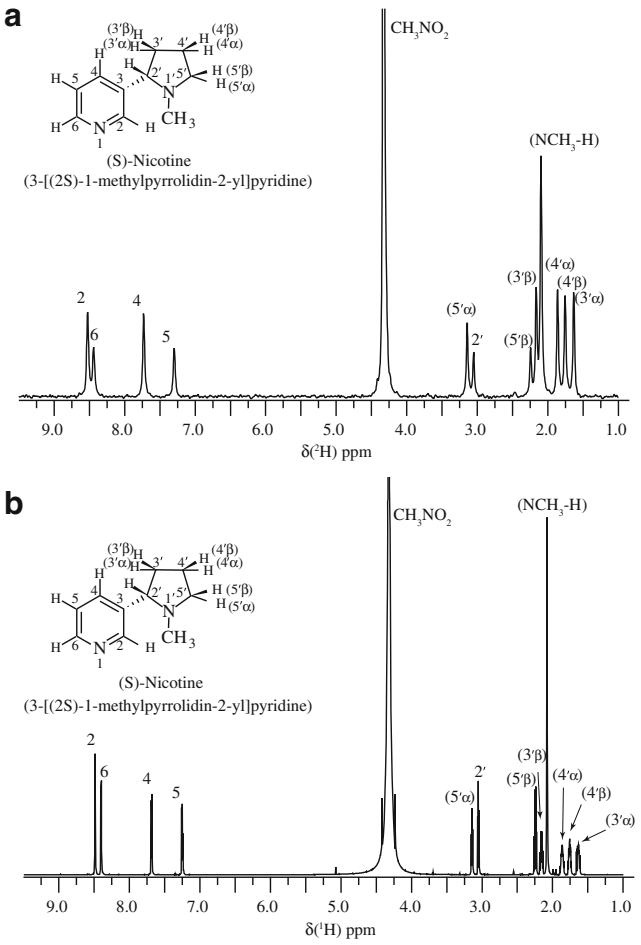

Fig. 1 Typical ^{2}H (**a**) and ^{1}H (**b**) NMR spectra of (S)-Nicotine. Site labels of (S)-Nicotine on the upper left are annotated according to IUPAC nomenclature

Data analysis

Multivariate data analysis was performed using SIMCA-P software (version 14.1, Umetrics AB, Umea, Sweden).

Orthogonal partial least-squares discriminant analysis (OPLS-DA) model [26] was built on the Pareto scaled experimental data to maximize the identification between natural and synthetic nicotine samples. The quality of the model was described by R^2 and Q^2 values. R^2 is defined as the proportion of variance in the data explained by the models and indicates goodness of fit, and Q^2 is defined as the proportion of variance in the data predictable by the model and indicates predictability. Univariate data analysis was performed using the publicly available statistical package "XCMS" [27]. The statistical significance of each site was analyzed by independent samples *t* test of the SPIR values of the natural and synthetic groups. The fold change was calculated by taking the ratio of the average of the SPIR values of the synthetic group by the average of those of the natural group. In case where fold change was smaller than 1, it was replaced by its negative inverse [28]. The SPIR values of adulterated mixture at the relevant sites, which are significantly responsible for differentiating natural and synthetic nicotine, can be presented in three-dimensional scatter plot using MATLAB software (2016a, MathWorks, Natick, MA) for visual detection of adulteration.

Results and discussion

Figure 1 shows the representative ^{2}H and ^{1}H NMR spectra of the nicotine samples. The proton-decoupled ^{2}H spectrum of nicotine consists of 12 distinct peaks which have the same chemical shifts as the corresponding signals in ^{1}H spectrum have. Site labels of nicotine on the upper left in Fig. 1 are annotated according to the IUPAC nomenclature of (S)-Nicotine. Assignments of sites 4 and 5 were swapped with respect to signal assignments of nicotine reported before [15] (labeled as sites 3 and 4 in the reference), based on the J couplings of ~ 4.77 Hz between sites 6 and 4 observed in ^{1}H spectrum of nicotine.

^{2}H/^{1}H NMR SPIR values of natural and synthetic nicotine

The ^{2}H/^{1}H NMR SPIR values of 5 nicotine samples (see Electronic Supplementary Material (ESM) Tables S1–S5) were derived from ^{1}H and ^{2}H NMR spectra (Fig. 2). The ^{2}H/^{1}H NMR SPIR values are shown to be independent of the sample concentrations, as demonstrated with *p*-Nicotine and the 2× *p*-Nicotine samples, which have nearly the same SPIR values.

Experimental results showed generally slightly higher ^{2}H/^{1}H SPIR values except for site 5′α in the synthetic origins ((R)- and *rac*-Nicotine) than in the natural nicotine (*p*- and (S)-Nicotine) samples, which appears to be in agreement with the results previously reported by Bernard Toulemonde [8] and

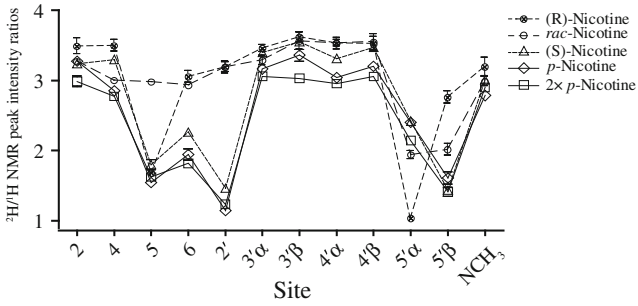

Fig. 2 The ^{2}H/^{1}H NMR SPIR values of 5 nicotine samples. Average SPIR values of all independently processed results are used in the plot and the range of measurement deviation is omitted for clarity

Gerald Remaud [10], where a more depleted ^{2}H/^{1}H isotopic ratio was observed in natural vanillin and benzaldehyde. The more ^{2}H enriched values for the synthetically derived products indicate that difference of ^{2}H/^{1}H isotopic ratios may be exploited to differentiate synthetic from natural compounds by measuring the ^{2}H/^{1}H SPIR values.

Difference of site-specific isotope fractionation of nicotine

The difference of site-specific isotope fractionation of natural nicotine from that of synthetic nicotine could be traced back to the different origins of the hydrogen atoms in the process of biosynthesis or chemical synthesis of nicotine. Nicotine is composed of two heterocyclic rings: a five-member pyrrolidine and a six-member pyridine ring. For the biosynthesis of the pyridine ring [14, 29], glucose is first converted to glyceraldehyde-3-phosphate in the process of glycolysis; subsequently, α-iminosuccinic acid produced by oxidization of aspartate with aspartate oxidase is condensed with glyceraldehyde-3-phosphate and cyclized by quinolinic acid synthase, yielding quinolinic acid, which contains a pyridine ring; the next reaction is the formation of nicotinic acid mononucleotide from quinolinic acid and phosphoribosyl pyrophosphate by quinolinic acid phosphoribosyl transferase (QPT); then, nicotinic acid mononucleotide is converted to NAD and nicotinic acid in subsequent cyclic steps. In the process above, glyceraldehyde-3-phosphate is proposed as precursor to offer the hydrogen atoms at sites 6 and 5 of pyridine ring, which were derived initially from the hydrogen atoms at sites (1 or 6) and (2 or 5) of glucose, respectively [30]. Ignoring the bias of non-quantitative NMR on the signal intensity (note, it is about precision, not the accuracy of real isotope ratio), which is in fact almost negligible, the lower value of ^{2}H/^{1}H NMR peak intensity ratios observed for sites 6 and 5 of natural nicotine corresponds to a lower ^{2}H/^{1}H isotopic ratio at sites (1 or 6, 6′) and sites (2 or 5) of glucose, respectively, compared with the site 4 of nicotine and sites (3 or 4) of glucose. The site-specific distribution of deuterium in glucose has been previously reported [30].

The pyrrolidine ring is derived from ornithine via the symmetric diamine putrescine [14, 31, 32]. Putrescine is first formed directly from ornithine by decarboxylation catalyzed by ornithine decarboxylase (ODC); then, putrescine is converted to N-methylputrescine through S-adenosylmethionine (SAM)-dependent N-methylation catalyzed by putrescine N-methyltransferase (PMT); finally, N-methylputrescine is oxidatively deaminated by N-methylputrescine oxidase (MPO) to 4-methylaminobutanal, which spontaneously decarboxylates and cyclizes to N-methyl-Δ-pyrrolinium cation. The pyrrolinium cation is ready for coupling with pyridine ring to generate nicotine. Sites 2′ and 5′α and 5′β in the pyrrolidine ring of nicotine arise from C2 or C5 atoms of ornithine. The lower values of $^{2}H/^{1}H$ NMR peak intensity ratios at sites 2′ and 5′β may be explained by the strong kinetic isotope effects in the course of hydrogen transfer after decarboxylation in the first and third steps, with NADPH or water as the hydrogen donor [14].

In terms of chemical synthesis, since the first synthetic nicotine by Pictet in 1904 [33], plenty of clever syntheses have been reported [21, 22, 34]. Different starting reactants or synthetic pathway will result in different $^{2}H/^{1}H$ isotopic ratios. In addition, kinetic and equilibrium isotope fractionation also affect $^{2}H/^{1}H$ isotopic ratio. Generally, biological processes are more susceptive to "kinetic" isotope fractionation. Organisms preferentially use lighter isotopic species because "energy costs" are lower [35–37]. In contrast, for chemical synthesis, equilibrium isotope fractionation is to distribute isotopes between two or more substances in chemical equilibrium. Most equilibrium fractionations are thought to result from the reduced vibrational energy (especially zero-point energy) when a heavier isotope replaced a lighter one, resulting in higher concentrations of the heavier isotopes in substances where the vibrational energy is most sensitive to isotope substitution [36–39]. Different mechanisms of the kinetic and equilibrium isotope fractionation can also explain why the values of $^{2}H/^{1}H$ SPIR of the synthetic nicotine are generally slightly higher than those of the natural nicotine, as shown in our experimental results.

To this end, on one hand, the site-specific $^{2}H/^{1}H$ isotopic ratio at a given molecular site depends on that of the corresponding position in the precursor or reactant. The precursor or reactant can be very different for biosynthesis or chemical synthesis; on the other hand, different effect of isotopic fractionation, mainly including kinetic fractionation and equilibrium fractionation, in biological system or chemical reaction, may also result in a different site-specific $^{2}H/^{1}H$ isotopic ratio of the same product. It is thus not surprising that distinct values of $^{2}H/^{1}H$ SPIR between natural and synthetic nicotine were observed in our experiments.

Multivariate and univariate data analyses of the $^{2}H/^{1}H$ NMR SPIR values of natural and synthetic nicotine samples

The experimentally measured values of SPIR at 12 distinct sites of natural and synthetic nicotine samples were Pareto scaled and OPLS-DA model (R^2X of 0.836, R^2Y of 0.993 and Q^2 of 0.991) was built on the preprocessed data. In Fig. 3a, OPLS-DA score plot showed clear differentiation between natural and synthetic groups. It indicates that some of the measured SPIR values could be significantly different between the two groups. The predictive component of OPLS-DA model explained 62.4% of the total variance and was sufficient to differentiate natural from synthetic groups (Fig. 3a). Sites 5, 6, 2′, 5′α, and 5′β of nicotine were found to be apart from others in the loading plot (Fig. 3b), which suggests they may be the potential discriminant features for the nicotine origin authentication. That is, the measured SPIR values (or essential SNIF) at these sites were significantly different between the natural and synthetic nicotine samples. Our results were in good agreement with the previously published results measured by conventional SNIF-NMR (that is, by IRMS together with quantitative ^{2}H NMR) [15], in which the SNIF values of ^{2}H to ^{1}H at these sites were most sensitive to the biosynthetic process.

The significance of the changes of SPIR values at 12 distinct sites between natural and synthetic nicotine was further evaluated by independent samples *t* test and the fold changes. Table 1 shows the statistical significance of multivariate and univariate data analyses of the SPIR values at 12 distinct sites of nicotine. After jointly filtered with variable importance in

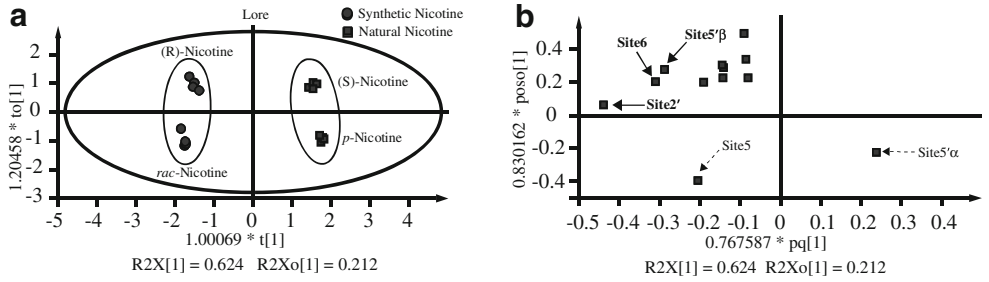

Fig. 3 OPLS-DA analysis of SPIR values at 12 distinct sites of natural and synthetic nicotine samples. (**a**) Score scatter plot (■ Natural Nicotine, including (S)- and *p*-Nicotine samples; ● Synthetic Nicotine, including (R)- and *rac*-Nicotine samples). (**b**) Loading plot

Table 1 Summary of the statistical significance of multivariate and univariate data analyses of the SPIR values at 12 distinct sites of nicotine (statistically most discriminant sites for differentiating natural and synthetic nicotine are shown in italic)

Site ID	^{1}H chemical shifts (ppm)	VIP	*p*(corr)	Fold change	*p* value
Site 2′	*3.05*	*1.853*	*− 0.997*	*2.358*	*6.910E−13*
Site 6	*8.44*	*1.328*	*− 0.951*	*1.464*	*2.920E−06*
Site 5′β	*2.25*	*1.262*	*− 0.847*	*1.674*	*2.460E−04*
Site 5′α	3.14	1.038	0.717	− 1.536	1.995E−03
Site 5	7.30	0.993	− 0.601	1.359	4.080E−02
Site 4′α	1.86	0.838	− 0.849	1.125	5.640E−04
Site 4	7.73	0.719	− 0.376	1.069	1.525E−01
Site 3′β	2.16	0.716	− 0.639	1.089	2.124E−02
Site 2	8.52	0.695	− 0.714	1.085	2.260E−03
Site 4′β	1.76	0.663	− 0.677	1.082	1.214E−02
Site 3′α	1.63	0.549	− 0.466	1.044	8.741E−02
Site NCH_3	2.10	0.438	− 0.493	1.044	3.934E−02

projection (VIP) > 1.0, OPLS coefficients (|*p*(corr)|) > 0.8, |fold change| > 1.2, and *p* value of *t* test < 0.05, sites 6, 2′, and 5′β were elucidated as the most discriminant sites which are responsible for differentiating natural and synthetic nicotine. Generally, VIP values larger than 1 indicate the most relevant variables, and VIP values below 0.5 are considered irrelevant variables [40]. *p* value of *t* test of certain sites smaller than 0.05 indicates a statistically meaningful difference between the average values of the natural and synthetic groups. Besides, sites 5 and 5′α respectively contribute to distinguishing *rac*-Nicotine or R-Nicotine from natural nicotine (Fig. 2). It illustrates that ^{2}H/^{1}H isotopic ratios of different synthetic nicotine samples may vary from each other due to different starting reactants or synthetic pathways.

Detection of adulterated mixture of natural nicotine with 20% synthetic nicotine

The distribution of SPIR values of natural, synthetic, and adulterated nicotine was illustrated in three-dimensional plot of the three most discriminant sites 6, 2′, and 5′β (Fig. 4). It reveals that, even with a relatively low level of adulterated synthetic nicotine (~ 20%), the adulterated sample can be visually clearly separated from the natural *p*-Nicotine, and also the synthetic *rac*-Nicotine in the three-dimensional scatter plot. However, it was considered to be challenging to detect such a low level of adulteration on the basis of the overall deuterium content determined by IRMS techniques.

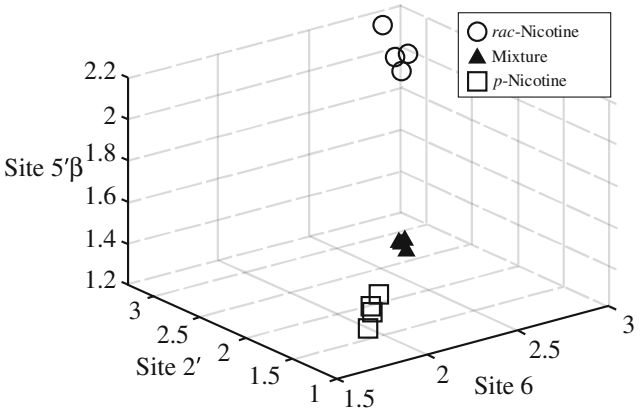

Fig. 4 Scatter plot of SPIR values in three-dimensional space of sites 6, 2′, and 5′β for class discrimination and adulteration detection

Conclusion

Isotopic measurement has been demonstrated to be the most effective method to detect small differences in the natural abundance of isotope composition at specific molecular sites. By measuring the ^{2}H/^{1}H NMR SPIR values of 4 different kinds of nicotine samples together with OPLS-DA analysis, differences in the isotopic composition of nicotine from different chemical or biochemical origins can be unambiguously detected. Even adulterated with a relatively low amount of synthetic nicotine in natural nicotine, the adulterated mixture can likely be unambiguously identified from the 100% natural nicotine. ^{1}H and ^{2}H NMR spectra can be collected in non-quantitative way and the ^{2}H/^{1}H SPIR values can be easily calculated from the measured ^{2}H and ^{1}H peak intensities, without the need of an additional IRMS spectrometer for the overall ^{2}H/^{1}H isotopic ratio determination. We propose that the method of ^{2}H/^{1}H SPIR values measured solely by NMR could be applied to elucidate an origin from a set of nicotine of unknown origins, which can be an attractive alternative tool for tobacco authentication. It can be expected that the SPIR values measured by NMR can also be widely used for the food product authentication and adulteration detection.

Acknowledgments The authors are grateful to Dr. Yaning Fu for providing the nicotine samples.

Funding information This work was supported by the National Key Research and Development Program of China (No. 2017YFC0906900), the National Natural Science Foundation of China (Nos. 21573258, 21505142), and Yunnan Provincial Science and Technology Department (No. 2015FA028).

Compliance with ethical standards

Conflict of interest The authors declare that they have no conflict of interest.

References

1. Brenna JT, Corso TN, Tobias HJ, Caimi RJ. High-precision continuous-flow isotope ratio mass spectrometry. Mass Spectrom Rev. 1997;16(6):382. https://doi.org/10.1002/(SICI)1098-2787(1997)16:5<227::AID-MAS1>3.0.CO;2-J.
2. Hilkert AW, Douthitt CB, Schlüter HJ, Brand WA. Isotope ratio monitoring gas chromatography/mass spectrometry of D/H by high temperature conversion isotope ratio mass spectrometry. Rapid Commun Mass Spectrom. 1999;13(13):1226–30. https://doi.org/10.1002/(SICI)1097-0231(19990715)13:13<1226::AID-RCM575>3.0.CO;2-9.
3. Meier-Augenstein W. Applied gas chromatography coupled to isotope ratio mass spectrometry. J Chromatogr A. 1999;842(1–2):351–71. https://doi.org/10.1016/S0021-9673(98)01057-7.
4. Muccio Z, Jackson GP. Isotope ratio mass spectrometry. Analyst. 2009;134(2):213–22. https://doi.org/10.1039/B808232D.
5. Tea I, Tcherkez G. Natural isotope abundance in metabolites: techniques and kinetic isotope effect measurement in plant, animal, and human tissues. Methods Enzymol. 2017;596:113–47. https://doi.org/10.1016/bs.mie.2017.07.020.
6. Martin GJ, Martin ML. Deuterium labelling at the natural abundance level as studied by high field quantitative ^{2}H NMR. Tetrahedron Lett. 1981;22(36):3525–8. https://doi.org/10.1016/S0040-4039(01)81948-1.
7. Remaud GS, Martin YL, Martin GG, Martin GJ. Detection of sophisticated adulterations of natural vanilla flavors and extracts: application of the SNIF-NMR method to vanillin and *p*-hydroxybenzaldehyde. J Agric Food Chem. 1997;45(3):859–66. https://doi.org/10.1021/jf960518f.
8. Toulemonde B, Horman I, Egli H, Derbesy M. Food-related applications of high-resolution NMR. Part II. Differentiation between natural and synthetic vanillin samples using ^{2}H-NMR. Helv Chim Acta. 1983;66(7):2342–5. https://doi.org/10.1002/hlca.19830660745.
9. Martin GJ. Multisite and multicomponent approach for the stable isotope analysis of aromas and essential oils. Acs Symp Ser. 1995;596:79–93. https://doi.org/10.1021/bk-1995-0596.ch008.
10. Remaud GS, Debon AA, Martin Y, Martin GG, Martin GJ. Authentication of bitter almond oil and cinnamon oil: application of the SNIF-NMR method to benzaldehyde. J Agric Food Chem. 1997;45(10):4042–8. https://doi.org/10.1021/jf970143d.
11. Martin GJ, Koziet J, Rossmann A, Dennis J. Site-specific natural isotópe fractionation in fruit juices determined by deuterium NMR an European inter-laboratory comparison study. Anal Chim Acta. 1996;321(2):137–46. https://doi.org/10.1016/0003-2670(95)00568-4.
12. Martin GJ, Martin ML. The site-specific natural isotope fractionation-NMR method applied to the study of wines. In: Linskens H-F, Jackson JF, editors. Wine analysis. Modern Methods of Plant Analysis, vol. 6. Berlin: Springer; 1988. p. 258–75. https://doi.org/10.1007/978-3-642-83340-3_9.
13. Martin GJ, Akoka S, Martin ML. SNIF-NMR—part 1: principles. In: Webb GA, editor. Modern magnetic resonance. Dordrecht: Springer; 2006. p. 1651–8. https://doi.org/10.1007/978-3-319-28388-3.
14. Shoji T, Hashimoto T. Biosynthesis and regulation of tobacco alkaloids. In: Wallner F, editor. Herbaceous plants: cultivation methods, grazing and enviromental impacts. New York: Nova Biomedical; 2013. p. 37–67.
15. Jamin E, Naulet N, Martin G. Multi-element and multi-site isotopic analysis of nicotine from tobacco leaves. Plant Cell Environ. 1997;20:589–99. https://doi.org/10.1111/j.1365-3040.1997.00099.x.
16. Chambers RP, Call GB, Meyer D, Smith J, Techau JA, Pearman K, et al. Nicotine increases lifespan and rescues olfactory and motor deficits in a Drosophila model of Parkinson's disease. Behav Brain Res. 2013;253:95–102. https://doi.org/10.1016/j.bbr.2013.07.020.
17. Quik M, Huang LZ, Parameswaran N, Bordia T, Campos C, Perez XA. Multiple roles for nicotine in Parkinson's disease. Biochem Pharmacol. 2009;78(7):677–85. https://doi.org/10.1016/j.bcp.2009.05.003.
18. Sanberg PR, Silver AA, Shytle RD, Philipp MK, Cahill DW, Fogelson HM, et al. Nicotine for the treatment of Tourette's syndrome. Pharmacol Ther. 1997;74(1):21–5. https://doi.org/10.1016/S0163-7258(96)00199-4.
19. Holladay MW, Lebold SA, Lin NH. Structure-activity relationships of nicotinic acetylcholine receptor agonists as potential treatments for dementia. Drug Dev Res. 1995;35:191–213. https://doi.org/10.1002/ddr.430350402.
20. Djordjevic MV, Doran KA. Nicotine content and delivery across tobacco products. In: Henningfield JE, London ED, Pogun S, editors. Nicotine psychopharmacology. Handbook of Experimental Pharmacology, vol. 192. Berlin: Springer; 2009. p. 61–82. https://doi.org/10.1007/978-3-540-69248-5_3.
21. Girard S, Robins RJ, Villiéras J, Lebreton J. A short and efficient synthesis of unnatural (*R*)-nicotine. Tetrahedron Lett. 2000;41(48):9245–9. https://doi.org/10.1016/S0040-4039(00)01675-0.
22. Welter C, Moreno RM, Streiff S, Helmchen G. Enantioselective synthesis of (+)(*R*)- and (−)(*S*)-nicotine based on Ir-catalysed allylic amination. Org Biomol Chem. 2005;3(18):3266–8. https://doi.org/10.1039/B508634E.
23. Willcott MR. MestRe Nova. J Am Chem Soc. 2009;131(36):13180. https://doi.org/10.1021/ja906709t.
24. Hu K, Westler WM, Markley JL. Simultaneous quantification and identification of individual chemicals in metabolite mixtures by two-dimensional extrapolated time-zero $^{1}H–^{13}C$ HSQC ($HSQC_0$). J Am Chem Soc. 2011;133(6):1662–5. https://doi.org/10.1021/ja1095304.
25. Li X, Hu K. Quantitative NMR studies of multiple compound mixtures. Annu Rep Nmr Spectrosc. 2017;90:85–143. https://doi.org/10.1016/bs.arnmr.2016.08.001.
26. Bylesjö M, Rantalainen M, Cloarec O, Nicholson JK, Holmes E, Trygg J. OPLS discriminant analysis: combining the strengths of PLS-DA and SIMCA classification. J Chemom. 2006;20(8–10):341–51. https://doi.org/10.1002/cem.1006.
27. Smith CA, Want EJ, O'Maille G, Abagyan R, Siuzdak G. XCMS: processing mass spectrometry data for metaboliteprofiling using nonlinear peakalignment, matching, and identification. Anal Chem. 2006;78(3):779–87. https://doi.org/10.1021/ac051437y.
28. Vinaixa M, Samino S, Saez I, Duran J, Guinovart JJ, Yanes O. A guideline to univariate statistical analysis for LC/MS-based untargeted metabolomics-derived data. Metabolites. 2012;2(4):775–95. https://doi.org/10.3390/metabo2040775.
29. Plaxton WC. The organization and regulation of plant glycolysis. Annu Rev Plant Physiol Plant Mol Biol. 1996;47(1):185–214. https://doi.org/10.1146/annurev.arplant.47.1.185.

30. Zhang BL, Quemerais B, Martin ML, Martin GJ, Williams JM. Determination of the natural deuterium distribution in glucose from plants having different photosynthetic pathways. Phytochem Anal. 1994;5:105–10. https://doi.org/10.1002/pca.2800050304.
31. Imanishi S, Hashizume K, Nakakita M, Kojima H, Matsubayashi Y, Hashimoto T, et al. Differential induction by methyl jasmonate of genes encoding ornithine decarboxylase and other enzymes involved in nicotine biosynthesis in tobacco cell cultures. Plant Mol Biol. 1998;38(6):1101–11. https://doi.org/10.1023/A:1006058700949.
32. Sandmeier E, Hale T, Christen P. Multiple evolutionary origin of pyridoxal-5′-phosphate-dependent amino acid decarboxylases. Eur J Biochem. 1994;221:997–1002. https://doi.org/10.1111/j.1432-1033.1994.tb18816.x.
33. Whidby JF, Seeman J. The configuration of nicotine. A nuclear magnetic resonance study. J Org Chem. 1976;41:1585–90. https://doi.org/10.1021/jo00871a022.
34. Huang K, Ortiz-Marciales M, De Jesús M, Stepanenko V. A new and efficient approach to the synthesis of nicotine and anabasine analogues. J Heterocyclic Chem. 2009;46(6):1252–8. https://doi.org/10.1002/jhet.233.
35. Limbach HH. Dynamic nmr spectroscopy in the presence of kinetic hydrogen/deuterium isotope effects. In: Deuterium and shift calculation. NMR Basic Principles and Progress, vol 23. Deuterium and Shift Calculation. Berlin: Springer; 1990. p. 63–164. https://doi.org/10.1007/978-3-642-75932-1_2.
36. Kendall C, Caldwell EA. Fundamentals of isotope geochemistry. In: Kendall C, McDonnell JJ, editors. Isotope tracers in catchment hydrology. Amsterdam: Elsevier; 1998. p. 51–86. https://doi.org/10.1016/B978-0-444-81546-0.50009-4.
37. Maggi F, Riley WJ. Mathematical treatment of isotopologue and isotopomer speciation and fractionation in biochemical kinetics. Geochim Cosmochim Acta. 2010;74(6):1823–35. https://doi.org/10.1016/j.gca.2009.12.021.
38. Urey HC. The thermodynamic properties of isotopic substances. J Chem Soc. 1947:562–81. https://doi.org/10.1039/jr9470000562.
39. Chacko T, Horita DRC. Equilibrium oxygen, hydrogen and carbon isotope fractionation factors applicable to geologic systems. Rev Mineral Geochem. 2001;43:1–81. https://doi.org/10.2138/rmg.2016.81.00.
40. Galindo-Prieto B, Eriksson L, Trygg J. Variable influence on projection (VIP) for orthogonal projections to latent structures (OPLS). J Chemom. 2014;28(8):623–32. https://doi.org/10.1002/cem.2627.